USP14 haploinsufficiency ameliorates Alzheimer's disease-like pathology in APP/PS1 mice

Hua Xu
Guangzhou Medical University
Xueheng Wu
Guangzhou Medical University
Lu Liang
Guangzhou Medical University
Haoyu Chen
Guangzhou Medical University
Jia Xu
Guangzhou Medical University
Wanyan Hu
Guangzhou Medical University
Xinci Li
Guangzhou Medical University
Qin Liu
Guangzhou Medical University
Xuejun Wang
University of South Dakota
Chang-E Zhang
Guangzhou Medical University
Jinbao Liu (jliu@gzhmu.edu.cn)
Guangzhou Medical University https://orcid.org/0000-0003-2220-2407

Research

Keywords: Alzheimer's disease (AD), USP14, Tau, Aβ, UPS

Posted Date: October 7th, 2020

DOI: https://doi.org/10.21203/rs.3.rs-84968/v1

Abstract

Background: Alzheimer's disease (AD) is the most common cause of dementia; its main pathological features are neurofibrillary tangles (NFTs) consisting of hyperphosphorylated microtubule-associated protein (Tau) in the cell and extracellular beta-amyloid protein (Aβ)-based senile plaques (SP). The ubiquitin-proteasome system (UPS) is the main pathway for protein degradation in cells. Proteasome malfunction exists in AD patients and may promote the progression of the disease. USP14 is a deubiquitinating enzyme associated with the 19S proteasome. Functional inhibition of USP14 was shown to enhance proteasome proteolytic function, but no reported study has investigated the impact of genetic inhibition of USP14 on AD.

Methods: Mice with heterozygous knockout of the *Usp14* gene ($USP14^{+/-}$) were generated and cross-bred with the APP/PS1 transgenic mice, the resultant offspring littermates were subjected to basal survival and growth analyses, and comparison of AD-like pathologies as detected with biochemical and histopathological methods and of cognitive function as assessed with the Morris water maze tests.

Results:USP14 mRNA and protein levels in $USP14^{+/-}$ mice were decreased by ~50% compared with $USP14^{+/+}$mice. The increases of total, K48 or K63 linked ubiquitinated proteins in APP/PS1 mouse brains were abolished in APP/PS1::$USP14^{+/-}$ mice. The increases in Aβ deposition and AD-associated phosphorylated Tau, senile plagues and neurofibrillary tangles, as well as spatial learning and memory decline induced by APP/PS1 were significantly attenuated in APP/PS1 mice.

Conclusions: This study demonstrates that global knocking down USP14 protein expression by 50% is tolerable by mice and exhibits marked protection against AD-like pathologies in a widely used AD mouse model, favoring the exploration of moderate inhibition ofUSP14 as a potentially novel and viable therapy against AD.

Background

Alzheimer's disease (AD) is a progressive neurodegenerative disease that is characterized by irreversible progressive cognitive deficits and extensive brain damage. Its main pathological features include neurofibrillary tangles (NFTs) consisting of the hyperphosphorylation of the microtubule-associated protein (Tau) in the cell and extracellular beta-amyloid protein (A-beta) based senile plaques (SP)[1, 2].

The ubiquitin-proteasome system (UPS) is the most important proteolytic pathway in eukaryotic cells. In UPS-mediated proteolysis, ubiquitination marks the substrate for degradation by the 26S proteasome, confers the substrate selectivity of this protein degradation mechanism, and has long been assumed as the rate-limiting step. However, recent advances in cell biology have revealed that the functionality of the 26S proteasome is highly regulated and can dictate the fate and degradation efficiency of a ubiquitinated substrate upon its arrival at the proteasome [3, 4]. By selective degradation of normal but no longer needed proteins, the UPS regulates cell cycle progression, cell survival, proliferation, apoptosis and other

key cellular pathways[5, 6]. By targeted degradation of terminally misfolded proteins, the UPS plays a pivotal role in protein quality control in the cell.

UPS impairment can occur in various conditions. The activity of proteasomes is reduced with aging process *in vitro* [7]. Proteasome function in AD patients' brains was impaired [8]. Reduction of proteasomal chymotrypsin-like activities was observed in the brain including hippocampus of AD animal models [9]. It is believed that the UPS can degrade APP proteins in the brain [10], and reduce the accumulation of extracellular amyloid proteins by regulating the production and the degradation of Aβ [11, 12]. Biochemical and morphological examinations of the brain of AD patients showed that phosphorylated Tau oligomer proteins accumulated on both sides of the synapse where ubiquitinated proteins, proteasome components and related chaperone proteins were also enriched, implicating that synaptic Tau protein aberrant aggregation may be an important mediator of proteotoxicity responsible for synaptic malfunction in AD [13]. There is reported evidence that both phosphorylated and non-phosphorylated Tau proteins are degraded by the non-ATP-dependent 20S proteasomes and the ATP-dependent 26S proteasomes [14, 15]. Taken together, these prior reports strongly suggest that UPS impairment may be a underlying cause for both Aβ deposition and Tau accumulation, two pathogenic tenets of AD.

The 26S proteasome complex consists of a 20S core particle (CP) and the 19S regulatory particle (RP) that caps the 20S at one or both ends. The 19S proteasome in mammals is associated with three deubiquitinating enzymes (DUBs): RPN11(Regulatory particle non-ATPase 11), UCHL5 (Ubiquitin carboxyl-terminal hydrolase isozyme L5) and USP14 (ubiquitin-specific protease 14). Among these proteasomal DUBs, RPN11 is the stoichiometric DUB subunit of the 19S proteasome and its removal of the ubiquitin (Ub) chain *en bloc* from a ubiquitinated protein is directly coupled to the subsequent degradation of the substrate protein while recycling Ub. USP14 and UCHL5, however, are reversibly associated with only a subset of 19S proteasomes and their deubiquitination may impact on UPS-mediated protein degradation in a manner different from RPN11 and from each other[16].

The association of USP14 with the proteasome is through the binding of its N-terminal ubiquitin-like domain (UBL) to the T2 site of RPN1 in the lid of the 19S proteasome.The binding of USP14 to the proteasome drastically increases USP14 DUB activity. This DUB activity resides in the USP domain at the C-terminus of USP14. Like RPN11, USP14 removes Ub chains *en bloc* from substrates; in other words, USP14's DUB activity breaks the isopeptidyl bond between a Ub chain and the substrate protein, giving rise to the deubiquitinated substrate protein molecule and the Ub chain, and the latter will be cleaved to individual Ub molecules by other DUBs. However, there are at least two major differences between USP14 and RNP11. First, RPN11-mediated deubiquitination is rigorously coupled to the commitment of the substrate protein to subsequent proteasomal degradation and is ATP-dependent, but USP14-mediated DUB activity is not linked to ATP binding and does not necessarily commit the substrate protein to subsequent degradation; second, USP14 seems to exert DUB activity only toward a substrate that is multi-ubiquitinated; and this theory posits that USP14 binds to one Ub chain and then removes other Ub chains on the same substrate protein molecule [17]. In terms of the effect of USP14-mediated DUB activity on

proteasomal degradation of its substrate proteins, published biochemical and cell biology studies have painted a rather muddy picture; both inhibitory and facilitative effects have been reported, seemingly to be substrate-dependent [16–19]. Small molecular inhibitors of USP14 DUB activity, IU1 and its derivatives IU1-47, were shown to promote proteasomal degradation of many proteotoxic proteins within cultured cells, including those associated with neurodegenerative diseases such as TDP-43 (TAR DNA-binding protein 43), ATXN3 (Ataxin 3), prion protein, and Tau [20–22], suggesting that USP14 inhibition may be explored as a therapeutic strategy for neurodegenerative diseases. However, tests using IU1 in animal models have yielded mixed results. Consistent with promotion of proteasomal degradation of damaged proteins by USP14 inhibition, IU1 and exosomal miR124, both suppress USP14, were shown to protect against cerebral ischemia/reperfusion injury in mice [23, 24], but USP14 inhibition was also shown to induce cell death and effectively treat malignancies in animal models [25, 26]. Moreover, the axJ mouse that is homozygous for an apparently loss-of-function mutation of *Usp14* and with a reduction of USP14 protein by 95%, shows severe neuromuscular abnormalities at 2–3 weeks and dies between 6–10 weeks of age [27]. Hence, we hypothesize that severe inhibition of USP14 (i.e., nearly 100%) is detrimental to at least the neuromuscular system whereas a moderate inhibition of USP14 might be benign and benefit the treatment of disease with increased proteotoxic stress via facilitating proteasomal degradation of the disease-causing proteins.

We conducted the present study to test this hypothesis. We created a new mouse model of USP-targeting allele and found homozygous USP14 knockout is mostly embryonic lethal but heterozygotes are viable and fertile and show no gross abnormalities. More interestingly, we were able to demonstrate that the USP14 heterozygous knockout or USP14 haploinsufficiency displays a protective effect on the AD-like pathology and cognitive decline in the APP/PS1 mouse model.

Materials And Methods

Study Design

The objective of our study was to determine whether USP14 plays a role in late-stage AD pathological characteristics and cognitive decline. We crossbred APP/PS1 transgenic mice, a widely used AD-like mouse model, with our newly created USP14$^{+/-}$ mice and aged the offspring to 12 months of age. The APP/PS1::USP14$^{+/-}$ mice were compared to APP/PS1, WT, and USP14$^{+/-}$ mice in terms of behavioral, neuropathological, and biochemical end points. Operators were blinded to mouse genotype for all outcome measures. We used power analysis for the Morris water test, the outcome measure with the highest variability, to compare cognitive behavior between 12-month-old APP/PS1::USP14$^{+/-}$ mice and APP/PS1 littermates and determined that we needed a minimum of 10 mice per group to achieve a statistical power of 80% for the $\alpha = 0.05$. To improve the rigor of the study, we included WT (n = 13), APP/PS1 (n = 9), APP/PS1::USP14$^{+/-}$ (n = 8), and USP14$^{+/-}$ (n = 12) for behavioral tests and n = 3 to 6 mice per group for biochemical and immunohistochemical tests.

Generation of USP14$^{+/-}$ mice and APP/PS1 mice

The mice with heterozygous knockout of the *Usp14* gene in the C57BL/6J inbred background ($Usp14^{+/-}$ mice) were generated through a contract to Shanghai Biomodel Organism Science &Technology Development Co., Ltd (Shanghai, China), using the CRISPR/Cas9 technology. In the knockout allele, the exon 5 of the *Usp14* gene is deleted.

APPswe/PS1dE9 mice (AKA, APP/PS1 mice)[28], $USP14^{+/-}$, and wild type (WT) C57BL/6J breeder mice were obtained from Shanghai Biomodel Organism Science &Technology Development Co., Ltd (Shanghai, China). WT, APP/PS1, $USP14^{+/-}$, and APP/PS1::$USP14^{+/-}$ littermates resulting from crossbreeding between hemizygous APP/PS1 mice and $USP14^{+/-}$ mice were used in this study.

The protocol for the care and use of all animals in this study was in accordance with the Guangdong Animal Center for the ethical treatment of animals and approved by the Institutional Animal Care and Use Committee of Guangzhou Medical University (SYXK2016-0168, Guangzhou, China). All mice were maintained in a temperature- and humidity-controlled room (22 ± 2 °C) and on a 12-h/12-h light/dark cycle. All animals had access to standard laboratory diet and drinking water *ad libitum*, and newborn mice were breastfed, and only males were used for this study to reduce gender-specific variability in the behavioral tests.

Genotype Detection

Mouse tails were clipped and DNA was extracted with an extraction kit (Takara Bio Inc, catalog #9170A), and the genotype was detected using DNA polymerase chain reaction (PCR). The following primers were used: 1. APP/PS1,internal positive control: 5’-CTA GGC CAC AGA ATT GAA AGA TCT-3’ (Forward), 5’-GTA GGT GGA AAT TCT AGC ATC ATC C-3’(Reverse); PS1: 5’-AAT AGA GAA CGG CAG GAG CA-3’ (Forward), 5’-GCC ATG AGG GCA CTA ATC AT-3’ (Reverse). 2. USP14:5’-TCC CAA AAT AAA TGT AAA GTC AAT-3’ (Forward),5’-AAG GTG GGT AGA GAA AAT AAA AGT-3’ (Reverse).

Morris Water Maze

The spatial memory was blindly evaluated by the Morris water maze test [29, 30]. Before each experiment, the mice were brought to the site to allow them to be acclimatized. The temperature of the room and the water was kept at 24 ± 2 °C. For spatial learning, the mice were trained to find a hidden platform for 6 consecutive days, 4 trials per day with a 20- to 30-second interval for each mouse from 3.00 to 8.00 p.m. On each trial, the mouse started from one of the four middle quadrants facing the wall of the pool and ended when the animal climbed on the platform. They were guided to the platform if they could not find the platform within 60 s. Through these training sessions, mice acquired spatial memory about the location of the safe platform. The swimming pathways and the latencies of the mice to find the hidden platform were recorded each day. The pathway and the length that the mouse passed through the previous platform quadrant were recorded by a video camera fixed to the ceiling of the room, 1.5 m from the water surface. The camera was connected to a digital-tracking device attached to an IBM computer loaded with the water maze software (Huaibei Zhenghua Biologic Apparatus Facilities). The spatial memory was tested 48 h later after the last training. When the platform was withdrawn, the path, distance

or time was recorded; the longer a mouse stayed in the target quadrant where previously the platform had been located, the better it scored for the spatial memory (the distance and the time traveled in the target quadrant and the escape latency were used to indicate the score).

Westernblot Analysis

Whole cell lysates and mouse cerebral cortex and hippocampal tissue homogenates were prepared in RIPA buffer (1 × PBS,1% NP-40, 0.5% sodium deoxycholate, 0.1% SDS) supplemented with 10 mM β-glycerophosphate, 1 mM sodiumorthovanadate,10 mM NaF,1 mM phenylmethylsulfonylfluoride (PMSF), and1 × Roche Complete Mini Protease Inhibitor Cocktail (Roche, Indianapolis,IN). SDS-PAGE, transferring,and immunodetection were performed as previously described [31]. In brief, equal amounts of total protein extracts were fractionated by12% SDS-PAGE and electrically transferred onto a polyvinylidenedifluoride (PVDF) membrane. Primary antibodies and appropriate horseradish peroxidase (HRP)-conjugated secondary antibodies were used to detect the designated proteins.The bound secondary antibodies on the PVDF membrane were reacted to the ECLdetection reagents (Santa Cruz, CA) and detected via exposing to X-ray films (Kodak,USA).

Enzymelinked Immunosorbent Assay (ELISA)

The hippocampus tissue was homogenized in RIPA buffer (Beyotime Biotechnology) containing a protease inhibitor cocktail (KeyGENBioTECH, catalog #KGP603), ultrasonicated, and centrifuged at 13000 g for 10 min. The supernatant was collected and total protein was measured with a Micro BCA protein assay (Pierce). Aβ40 and Aβ42 were separately measured with ELISA Kits (R□D system) by following manufacturer's instructions.

Quantitative reverse transcriptase (RT-) PCR (qRT-PCR)

Total RNA from brain tissues was isolated using the RNAiso Plus (Takara Bio Inc, catalog #9108). cDNA was prepared from the RNA using the PrimeScript™ RT reagent Kit with gDNA Eraser (Takara Bio Inc, catalog #RR047A). The real-time PCR amplification was performed using the SYBR Green method with SYBR Premix Ex TaqTM II (Takara Bio Inc, catalog #RR820A), and according to manufacturers' instructions.

The following primers were used: APP: 5'- GCC AAC CAG CCA GTG ACC ATC-3 (forward), 5'-GCG ACG GTG TGC CAG TGA AG-3' (reverse); PS2: 5'-CTG GCA ACG GAG ACT GGA ACAC-3'(forward), 5'-TGA ACA CAG CAA GCA GCA GGA G-3' (reverse); USP14:5'- AAA CTT CTT CTA GTA TCC CAC C-3' (forward); 5'- TGC TGA AGA TAC TGC CCT T -3' (reverse); MAPT(Tau):5'-ACT CTG CTC CAA GAC CAA – 3' (forward), 5'- TCG GCT GTA ATT CCT TCT G -3'(reverse);β-actin:5'- GCT GTG CTA TGT TGC TCT A -3' (forward), 5'- CGT TGC CAA TAG TGA TGA C -3' (reverse). Results were normalized against the internal control using the Δ-ΔCTmethod.

Immunohistochemistry

Mice were anesthetized and transcardially perfused rapidly with 50 ml normal saline solution, followed by fixation *in situ via* perfusion for 20 min at 4 °C with Zamboni's solution containing 4% paraformaldehyde, 15% saturated picric acid, and 24 mM NaH2PO4/ 126 mM Na2HPO4 (pH7.2). The brain was removed from the skull of the fixed animals and post-fixed in the same Zamboni's solution for another 24 h at 4 °C. Then coronal slices (8–10 μm) were cut with a Vibratome (Leica, VT1000S, Germany).

The immunohistochemical procedures were as follows [29]: Sections were permeabilized with 0.3% H2O2 in absolute methanol for 10 min to block endogenous peroxidase, and non-specificsites were blocked with 5% bovine serum albumin (BSA) for 30 min at room temperature, and incubated with primary antibodies for 24 h at 4 °C. After washing with PBS, sections were subsequently incubated with biotin-labeled secondary antibodies for 1 h at 37 °C. The immunoreaction was detected using horseradish peroxidase-labeled streptavidin for 1 h at 37 °C and visualized with the DAB tetrachloride system for brown color. A negative control for every antibody was used with PBS, then observed under a light microscopy (Olympus BX60, Tokyo, Japan) and photographed. The IODs and plaque burden in each image and were counted and measured using Image-Pro Plus v 6.0 software (Media Cybernetics Inc, Bethesda, MD, USA).

Gallyas-Braak silver staining

Silver staining was performed as previously reported [32]. In brief, brain sections (10 μm) were mounted on glass slides, hydrated through a series of alcohol solutions, then subject sequentially to the following treatments:1) 0.3% KMnO4 10 min, then washed to water clarification; 2) 1% C2H2O4• 2H2O 2 min, and La(NO3)3 solution (1.15 mM La(NO3)3•6H2O, 14.7 mM CH3COONa•3H2O) 1 h, then washed 3 × 5 min; 3) alkaline AgI(0.1 M NaOH, 0.06 M KI, 1% AgNO3 35 ml) incubation 45minin at 37℃, avoided light, and the 1% acetic acid washing 3 × 1 min; 4) the developer solution (□:0.47 M Na2CO3;□:25 mM NH4NO3, 11.77 mM AgNO3, 3.5 mM H6O39SiW12; □: 25 mM NH4NO3, 11.77 mM AgNO3, 3.5 mM H6O39SiW12, 6.1 ml 40%HCHO; three solutions mixed equal parts, temporarily preparation and avoided light) incubated 30 min, then 1% acetic acid washed; 5) 0.5% AuCl3 30 s, and then washed 2 × 5 min; 6) 1% NaS3O3•5H2O fixed 1 min, and washed 10 min. Then generally dehydrated, hyalinized, sealed, and then examined and photographed using a microscope (Olympus BX60, Tokyo, Japan) equipped with a digital camera.The IODs in each image were counted and measured using Image-Pro Plus v6.0 software (Media Cybernetics Inc,Bethesda, MD, USA).

Thioflavin-S staining

Brain sections (10 μm thickness) mounted on glassslides were hydrated through a series of alcohol solutions, soaked in 0.3% KMnO4 for 4 min, followed by a wash with 1% oxalicacid for 1 min [33]. Next, the brain sections were incubated with 0.05% aqueous Thioflavine-S (SIGMA, catalog#T1892) dissolved in 50% ethyl alcohol for 8 min at room temperature in dark, then washed in 50% ethyl alcohol twice and subsequently in three exchanges of distilled water. The slides were then incubated in a high concentration of phosphate buffer (411 mM NaCl, 8.1 mM KCl, 30 mM Na2HPO4, 5.2 mM KH2PO4, pH 7.2) at 4℃ for 30 min, washed, and finally sealed in 10% glycerin with coverslips. The stained sections were stored in a

dark box at 4 °C before they were observed with a fluorescence microscope (Leica, Germany) and photographed.The plaque burden in each image were counted and measured using Image-Pro Plus v6.0 software (Media Cybernetics Inc, Bethesda, MD, USA).

Statistical analysis

Water maze data are expressed as mean ± SEM, others are expressed as mean ± SD. GraphPad Prism 7.0 software (GraphPad Software) was used for statistical analysis. Differences between two groups were evaluated for statistical significance using two-tailed Student's t-test. A difference among 3 or more groups, one-way ANOVA or when appropriate, 2-way ANOVA, followed by the Holm-Sidak test for pair-wise comparisons were performed. *P* value < 0.05 was considered statistically significant.

Result

Reduction of USP14 mRNA and protein levels in brain tissue of USP14$^{+/-}$ mice

Ataxia (axJ) mice with 95% reduction of USP14 proteins die within 2 months after birth [27]. Breeding between USP14$^{+/-}$ mice yielded the live birth of USP14$^{-/-}$ offspring at a frequency that is drastically lower than the Mendelian ratio, indicating that the overwhelming majority of homozygous global USP14 knockout embryos do not survive to term. The few USP14$^{-/-}$ embryos that survived to birth showed growth retardation and died within a few months. We then performed a comprehensive baseline characterization on the USP14$^{+/-}$ mice which are viable and fertile. qRT-PCR and Western blot analyses respectively showed that USP14 mRNA and protein levels were reduced by approximately 50% in the cerebral cortex of USP14$^{+/-}$ mice compared to wild-type mice (Fig. 1A ~ 1C). USP14$^{+/-}$ mice do not show any gross abnormalities in growth and general wellbeing or increased mortality compared with littermate WT mice (Fig. 1D and 1E). These results not only demonstrate that the germ-line targeting of the *Usp14* gene has succeeded but also indicate that the USP14$^{+/-}$ mice represent a valuable tool for studying the role of USP14 down-regulation in pathophysiology.

USP14 haploinsufficiency did not alter APP/PS1 mouse body weight and premature death

To test the effect of USP14 downregulation on AD, we crossbred USP14$^{+/-}$ mice with the APP/PS1 transgenic mice, which resulted in the following genotypes at the normal Mendelian ratio at birth: WT, APP/PS1, USP14$^{+/-}$, APP/PS1::USP14$^{+/-}$. Monitoring the time course of body weight changes during postnatal 48 weeks revealed no statistically significant difference in body growth among the four genotypes (Fig. 1D). And recording the premature death of these mice during postnatal 48 weeks detected no increases in premature death in USP14$^{+/-}$mice compared with the WT. Nonetheless, a significant increase in mouse premature death was observed in both APP/PS1 and APP/PS1::USP14$^{+/-}$ groups but the difference between the two groups is not statistically significant (Fig. 1E). We observed a mortality of nearly 40% in both APP/PS1 mice and APP/PS1::USP14$^{+/-}$ mice by 6 months of age, similar

to the APP/PS1 mouse mortality reported in the literature [34]. These findings indicate that the USP14 haploinsufficiency does not mitigate the early mortality of this AD mouse model.

Impact of USP14 haploinsufficiency on UPS function

Pharmacological inhibition of USP14 DUB activity was shown to promote UPS-mediated degradation of, at least, a subset of proteins[35]. Our team has reported that the simultaneous inhibition of USP14 and UCHL5 inhibits UPS proteolytic function and causes aberrant protein aggregation [36]. The K48-linked Ub chain is the most important type of Ub moieties that target the protein for degradation by the 26S proteasome. K63-Ub chains are the second largest class of Ub chains, participating in the regulation of signaling pathways and also functioning as a recognition signal for multiple autophagy receptors to guide the degradation of the modified proteins through autophagy [6]. To examine the effect of UPS14 haploinsufficiency on UPS functioning in mouse brains, we compared the steady state protein levels of Usp14 and Ub conjugates in the cerebral cortex of 12-month-old mice (Fig. 2). Western blot analyses detected comparable Usp14 protein levels between WT and APP/PS1 mice and a significantly lower Usp14 abundance in both USP14$^{+/-}$ and APP/PS1::USP14$^{+/-}$ mice compared with both WT and APP/PS1 mice. More interestingly, the total ubiquitinated proteins (Ub-prs), as well as K48-linked (K48-Ub) and K63-linked Ub (K63-Ub) were all significantly increased in APP/PS1 mice compared with WT mice, but the increases were significantly attenuated or even abolished when APP/PS1 was coupled with USP14$^{+/-}$. These results suggest that downregulation of USP14 improves the degradation of ubiquitinated proteins in brain tissues, which is consistent with improvement of proteasomal proteolysis by USP14 inhibition.

Effect of USP14 haploinsufficiency on APP and its related processing enzymes in APP/PS1 mice

APP is a transmembrane protein that can be hydrolyzed by the α-secretase pathway to produce soluble non-toxic fragments. It can also be cleaved by the β-secretase (BACE1) pathway and then hydrolyzed by γ-secretase (PS1, PS2) to produce fragments Aβ40 and Aβ42 containing 39 ~ 43 amino acid residues. It has been reported that abnormal phosphorylation of APP at Thr668 site can increase the affinity of APP to beta-secretase (BACE1), resulting in increased production of Aβ [37]. Therefore, we performed Western blot analyses for the total (APP) and Thr668-phosphorylated (pT668) APP, as well as BACE1, PS1, and PS2 in the cerebral cortex of mice at 12 months of age. The results showed that the marked increases of APP and pT668 in APP/PS1 mice were significantly attenuated by the downregulation of USP14. BACE1 was not changed and PS1 was increased while PS2 was reduced in APP/PS1 mice, but USP14 haploinsufficiency showed no discernible effects on any of them (Fig. 3A, B).

To determine whether the reduction of APP and p-Thr668-APP proteins by USP14 haploinsufficiency and the decreases of PS2 proteins in APP/PS1 mice resulted from a decrease in gene transcription, we performed RT-qPCR analyses for APP using the RNA from the cerebral cortex. The results showed that USP14 deficiency had no effect on the mRNA level of APP (Fig. 3C), which is consistent with the notion that the reduced APP protein content in APP/PS1::USP14$^{+/-}$ mice compared with the APP/PS1 mice is attributable to increased APP protein degradation. Similarly, RT-qPCR results showed no significant difference in PS2 mRNA levels between APP/PS1 and control mice (Fig. 3D), indicating that

overexpression of the mutant PS1 in the APP/PS2 mice may lead to excessive degradation of PS2 proteins.

Effect of USP14 haploinsufficiency on Aβ level in APP/PS1 mice

Senile plaques (SP) caused by the aggregation of Aβ areone of the main pathological features in AD. The APP/PS1 mice are a widely used transgenic mouse model of AD. To investigate whether downregulation of USP14 affects Aβ levels in AD brains, hippocampal proteins were extracted from 12-month-old APP/PS1 mice and the enzyme-linked immunosorbent assay (ELISA) was used to measure Aβ40 and Aβ42 levels. Our results showed that the hippocampal content of Aβ40 and Aβ42 were significantly lower in APP/PS1::USP14$^{+/-}$ mice than in APP/PS1 mice although both were higher than those in WT or USP14$^{+/-}$ mice ($p < 0.001$; Fig. 4A-B).

It has been reported that free Aβ is less toxic than aggregated Aβ, and only when forming amyloid plaques, Aβ causes neurotoxic inflammatory responses and oxidative stress. Hence, we also assessed Aβ deposits in brain tissues using Thioflavin-S staining and Aβ (MOAB2) antibody immunohistochemical staining. We found that, compared with the APP/PS1 group, the Aβ amyloid plaques in both the cerebralcortex and the hippocampus of the APP/PS1::USP14$^{+/-}$ group were significantly reduced ($p < 0.001$; Fig. 4C, 4D). These results indicate that USP14 haploinsufficiency can significantly reduce Aβ content and Aβ deposition in the cerebral cortex and hippocampus of the AD mice.

Effect of USP14 haploinsufficiency on Tau proteins in the brain of APP/PS1 mice

The main function of Tau proteins is to promote microtubule assembly in the axon. Phosphorylation of the Tau protein at multiple sites impairs its normal function and promotes its aggregation to form paired helical filaments (PHFs), causing neurofibrillary tangles (NFTs) [38, 39]. In the APP/PS1 mice, the increase of total Tau protein and hyperphosphorylation of multiple sites in Tau occur in the progression of AD although the specific underlying mechanism is unclear [40]. To determine whether the total Tau protein or phosphorylation levels of Tau in AD mice have changed and whether USP14 haploinsufficiency would alter these pathological features, we extracted RNA and total proteins from mouse hippocampal tissues to assess changes in Tau expression and Tau protein phosphorylation. qRT-PCR showed no significant differences in Tau mRNA (Fig. 5A) among the four groups. Western blot analyses showed that, compared with the WT or USP14$^{+/-}$group, the APP/PS1 group displayed significant increases in the total Tau (Tau-5) and in the Ser214-, Ser262-, or Ser396-phosphorylated Tau, as well as a significant decrease in Tau-1(i.e., Ser195/198/199/202 dephosphorylated Tau); and these changes were discernibly attenuated in the APP/PS1::USP14$^{+/-}$ group, compared with the APP/PS1 group ($p < 0.05$ or 0.01; Fig. 5B, 5C). No significant differences in the phosphorylation of Thr231-Tau (Fig. 5B, C) were discerned among the four groups. These results indicate that the increase in Tau protein is unlikely caused by increased expression but more than likely by decreased degradation; the attenuated accumulation of phosphorylated Tau in APP/PS1::USP14$^{+/-}$ mice is consistent with an improvement of proteasome proteolytic function by USP14 inhibition.

We then examined the distribution of Tau proteinsin the hippocampus using immunohistochemistry. Our results showed that the immunostaining density for Ser195/198/199/202 dephosphorylated Tau (Tau-1) was decreased and that for the Ser396-phosphorylated Tau was increased in the hippocampus of APP/PS1 mice; and these AD-like alterations were discernibly less pronounced in APP/PS1::USP14$^{+/-}$ mice ($p < 0.05$ or 0.01;Fig. 5D, 5E), consistent with the Western blot results. Taken together, AD-like Tau changes in APP/PS1 mice were significantly attenuated by USP14 haploinsufficiency.

The effect of USP14 haploinsufficiency on the senile plaques and neurofibrillary tangles in the brain of APP/PS1 mice

We further examined brain pathology using the modified Gallyas-Braak silver staining, a well-accepted method for detection of extracellular senile plaques, intracellular neurofibrillary tangles, and intracytoplasmic inclusions in glial cells in AD brain tissue [41]. The silver staining revealed striking senile plaques and darkening and entangling of nerve fibers in the brain of APP/PS1 mice; and these pathological changes were less severe in APP/PS1::USP14$^{+/-}$ mice (Fig. 6), indicating that USP14 downregulation ameliorates AD-like brain pathology in APP/PS1 mice.

Effects of USP14 haploinsufficiency on spatial learning and memory in APP/PS1 mice

We performed Morris water maze tests to evaluate the spatial learning and memory of 12-month-old APP/PS1 AD mice and the impact from USP14 haploinsufficiency. We observed that the swimming speed of each of the four groups did not differ significantly within the 6 days of test (Fig. 7A), indicating that the physical strength or exercise capacity of these mice is comparable. Over the 6-day training period, the escape latency measured daily in WT and USP14$^{+/-}$ mice showed similarly a gradual decrease from day 1 to day 6 but the slope of this decrease trajectory was less steep in the APP/PS1 group than in WT mice, and the slope of APP/PS1::USP14+/- mice fell in between those of APP/PS1 mice and WTmice (Fig. 6B). Consequently, the escape latency of APP/PS1 mice measured at day 6 was significantly prolonged compared with that of WT or USP14$^{+/-}$mice, but this prolongation was attenuated in the APP/PS1::USP14$^{+/-}$ mice (Fig. 7B, 7C), indicating that the spatial learning ability is impaired in APP/PS1 mice and this impairment is improved by downregulation of USP14. The memory ability was measured after the platform was withdrawn on the 8th day. The results showed that compared with the WT or USP14$^{+/-}$ mice, the APP/PS1 mice showed a significant reduction in the duration of residence and traveling distance in the quadrant of the platform, in the number of times passing across the platform, and in the distance traveled in the quadrant ($p < 0.001$); however, these reductions were significantly less pronounced in the APP/PS1::USP14$^{+/-}$ mice ($p < 0.05$; Fig. 7D-F), indicating that spatial memory is impaired in APP/PS1 mice but the impairment is improved by reduction of USP14 expression. These results indicate that USP14 haploinsufficiency can improve the spatial learning and memory ability of APP/PS1 mice.

Discussion

Small molecular inhibitors of USP14 DUB activities were shown to promote proteasomal degradation of a subset of proteins especially some of the pathogenic proteins in cultured cells at least [20, 21], making USP14 inhibition an attractive potential strategy to treat diseases with increased proteotoxic stress such as neurodegenerative diseases [19]. However, this strategy has rarely been tested in animal models. A major concern that discourages such a strategy was that USP14 inhibition might harm the nervous system because mice with a genetic mutation that leads to loss of 95% of USP14(e.g., ax^J mice) develop ataxia and show a markedly shortened lifespan [27]. Taking advantage of the newly created mouse model of USP14 haploinsufficiency, the present study demonstrates for the first time in animal models that a loss of 50% of USP14 can significantly attenuate the AD-like pathology (both senile plagues and neurofilament tangling) and the cognitive deficit in a commonly used AD mouse model, probably through facilitating the proteasomal degradation of APP and abnormal Tau proteins in the brain. These discoveries also provide *in vivo* evidence that supports the promoting effect of USP14 inhibition on proteasomal proteolytic function toward at least a subset of proteins. Hence, the findings of the present study suggest that a well-controlled extent of USP14 inhibition may benefit AD treatment.

Consistent with the significantly shorten lifespan of the ax^J mice[27], $USP14^{-/-}$ mice die either during embryonic phase or prematurely after birth, indicating that a complete loss of USP14 is lethal. However, despite 50% reduction in both mRNA and protein levels of Usp14 in $USP14^{+/-}$ mice, these mice do not show developmental or growth defects nor do they show abnormal neurological or cognitive phenotypes by 12 months of age, the oldest mice ever tested. These findings indicate that globally inhibiting USP14 activity by 50% is tolerable by mice, offering an opportunity to test the impact of a partial loss of USP14 on increased proteotoxicity in mice. Although the Kaplan-Meier survival curves were indistinguishable between APP/PS1::$USP14^{+/-}$ mice and APP/PS1 mice within at least the first 12 months of age, the spatial learning and memory deficits revealed by the Morris water maze tests were significantly milder in the APP/PS1::$USP14^{+/-}$ mice than in APP/PS1 mice at 12 months of age. This strongly suggests that reducing USP14 to 50% of its normal level not only is tolerated by the AD mice but also effectively treats their cognitive impairment. The improvement of neurological functions in AD mice by USP14 haploinsufficiency was associated with significantly less severe senile plagues and neurofilament entangles, indicate that USP14 inhibition probably suppresses directly the AD pathogenesis in the APP/PS1 mice. Notably, the time of mouse death in both the APP/PS1 group and the APP/PS1::$USP14^{+/-}$ group was all before 26 weeks of age, which is consistent with reported features of the APP/PS1 mice and also indicate that the premature death of the APP/PS1 mice is not due to amyloid deposition. This is because (1) amyloid deposition in this Ad mouse model is detectable between 4 to 6 months and becomes more pronounced at 12 months [28] but the mortality does not further increase after 26 weeks.

As the main protein degradation pathway in the cell, the UPS regulates proteolysis of most cellular proteins, both misfolded and native [6]. When UPS function is impaired, excessive or deleterious proteins cannot be selectively removed and thereby accumulate in the cell, which affects virtually all cellular processes and may contribute to the development of various diseases [42]. Ub-positive inclusion bodies are present in neurodegenerative disease-affected brains and are considered an important marker of

these diseases, including AD, Parkinson's disease, Huntington's disease, and amyotrophic lateral sclerosis [43]. Therefore, it is very likely that the beneficial effects of USP14 haploinsufficiency on APP/PS1 mice are through enhancing proteasomal proteolytic function and thereby increasing the degradation of abnormal proteins. Indeed, increases of total, K48- and K63-linked ubiquitinated proteins in the cerebral cortex of the AD mice were completely abolished by USP14 haploinsufficiency; and total APP and T668-phosphorylated APP proteins as well as the total Tau and most AD-linked phosphorylated Tau proteins in the cerebral cortex of APP/PS1 mice were significantly reduced by USP14 haploinsufficiency.

Overexpression of both the mutant APP and PS1 is obviously the primary cause of pathology in the APP/PS1 mice. Our data show that USP14 haploinsufficiency does not affect the APP mRNA levels or the protein levels of APP cleaving enzymes BACE1 and PS1 in the APP/PS1 mice; however, total APP and p-Thr668-APP protein levels were significantly lower in APP/PS1::USP14$^{+/-}$ mice compared with the APP/PS1 mice, suggesting that increased degradation of the APP plays an important role in the protection against AD-like pathology by USP14 haploinsufficiency, which is further supported by significantly lower levels of Aβ40 and Aβ42 in APP/PS1::USP14$^{+/-}$ mice compared with the APP/PS1 mice. Aβ40 and Aβ42 are the metabolic products of APP and especially Aβ42 is susceptible to aberrant aggregation, ultimately forming senile plagues in AD brains. Both immunohistochemical staining for Aβ and the Th-S staining revealed the amyloid plagues in the AD mouse brains were significantly reduced USP14 haploinsufficiency.

The Silver staining results further show attenuation of AD-associated NFTs by USP14 haploinsufficiency. This could conceivably result from reduced APP-based pathogenesis as discussed above. The main reason for APP/PS1 mice to be an AD model is that they are based on the pathological feature of increased Aβ production; and as the disease progresses, Tau hyperphosphorylation occurs in the brain of APP/PS1 mice [40]. Another potential mechanism underlying the attenuation of AD-associated NFTs by USP14$^{+/-}$ could be directly promoting the degradation of pathogenic Tau proteins as total Tau and AD-pathogenic species of phosphorylated Tau proteins but not Tau mRNA in the AD mouse brain were all significantly reduced by USP14 haploinsufficiency. Tau protein phosphorylation plays an important role in regulating its function, affecting the binding of Tau to microtubules, and then regulating the stability and assembly of microtubules themselves. Meanwhile, the highly phosphorylated Tau proteins also can aggregate to form PHFs, which in turn form NFTs [44]; this process can also be spread in brain tissue by a prion-like method to the whole brain [45]. In the brain of AD patients,Tau is phosphorylated at many sites; the most common are Tyr18, Ser198/199/202, Thr205, Thr231, Ser214, Ser262, Ser396/404, Ser422,etc. [38, 46]. It has been reported that Tau proteins are substrates for the UPS. Previous studies have shown that inhibition of USP14 can promote the degradation of Tau protein and the decrease of Tau phosphorylation level [20, 21, 47]. It has also been found that the inhibition of USP14 does not change the protein level of Tau, and even increases the level of Tau [48, 49]. These reports are contradictory and may be related to the degree of inhibition of USP14 activity and differences in experimental conditions. Hence, the mechanism by which USP14 haploinsufficiency reduces Tau proteins in AD brains remain to be defined in the future.

Conclusions

The present study shows that knocking down USP14 by 50% significantly alleviate AD-like pathologies, including amyloid deposition, NFTs, and recognitive decline,in a widely used AD mouse model. These beneficial effects from USP14 haploinsufficiency are perhaps attributable to the facilitation of proteasomal degradation of both mutant APP and the pathogenic Tau proteins in brain. These new *in vivo* findings provide a strong experimental demonstration that favors the exploration of a USP14 inhibition-based pharmaceutical strategy for treating AD.

Abbreviations

AD :Alzheimer's disease

NFTs :Neurofibrillary tangles

Tau: Microtubule-associated protein

Aβ: β-Amyloid

SP: Senile plaques

UPS: Ubiquitin-proteasome system

USP14: ubiquitin-specific protease 14

CP: Core particle

RP: regulatory particle

DUBs: Deubiquitinating enzymes

RPN11: Regulatory particle non-ATPase 11

UCHL5: Ubiquitin carboxyl-terminal hydrolase isozyme L5

Ub: Ubiquitin

APP: Amyloid precursor protein

PS1/2: Presenilins 1/2

UBL: Ubiquitin-like domain

TDP-43: TAR DNA-binding protein 43

ATXN3: Ataxin 3

PCR: Polymerase chain reaction

PVDF: polyvinylidenedifluoride

HRP: horseradish peroxidase

SDS: Sodium deoxycholate

PMSF: Phenylmethylsulfonylfluoride

RIPA: Radioimmunoprecipitation assay

qRT-PCR: Quantitative reverse transcriptase (RT-) PCR

BSA: bovine serum albumin

PBS: Phosphate Buffered Saline

IOD: Intensity of Optical density

WT: Wild type

BACE1: Beta-Site APP Cleaving Enzyme 1

PHFs: paired helical filaments

Ub-Prs.: Ubiquitinated proteins

Declarations

Acknowlegements

We thank Drs. Daolin Tang and Huabo Su for helpful discussions.

Funding

The study was supported in part by Guangzhou Education System Foundation (1201610014, 1201620494); the National Natural Science Foundation of China (81170608, 81570278, 81602427, 81600089, 81670156); the Science and Technology Program of Guangzhou (201707010046, 201604020001); The National Funds for Developing Local Colleges and Universities (B16056001); Natural Science Foundation research team of Guangdong Province (2018B030312001); Natural Science Foundation of Guangdong Province (2017A030313662).

Corresponding author

Correspondence to Jinbao Liu, Chang-e Zhang and Xuejun Wang.

Author contributions

J.L and C.E.Z. designed research studies, analyzed data, and wrote the manuscript. X.W wrote and revised the manuscript. H.X. performed experiments and drafted the manuscript. X. W., L. L., H. C., J. X., W. H., X.L., Q.L. assisted in conducting key experiments. All authors read and approved the final manuscript.

Availability of data and materials

All the data generated in the current studies will be made readily available from the corresponding authors upon reasonable request.

Ethics approval and consent to participate

The protocol for the care and use of all animals in this study was in accordance with the Guangdong Animal Center for the ethical treatment of animals and approved by the Institutional Animal Care and Use Committee of Guangzhou Medical University (SYXK2016-0168, Guangzhou, China).

Consent for publication

N/A.

Competing interests

Authors declare no conflict of interest.

References

1. **2018 Alzheimer's disease facts and figures.***Alzheimer's & Dementia* 2018, **14:**367-429.
2. Chai YL, Chong JR, Weng J, Howlett D, Halsey A, Lee JH, Attems J, Aarsland D, Francis PT, Chen CP, Lai MKP: **Lysosomal cathepsin D is upregulated in Alzheimer's disease neocortex and may be a marker for neurofibrillary degeneration.***Brain pathology (Zurich, Switzerland)* 2019, **29:**63-74.
3. Wang X, Wang H: **Priming the Proteasome to Protect against Proteotoxicity.***Trends Mol Med* 2020, **26:**639-648.
4. Collins GA, Goldberg AL: **The Logic of the 26S Proteasome.***Cell* 2017, **169:**792-806.
5. Finley D: **Recognition and processing of ubiquitin-protein conjugates by the proteasome.***Annual review of biochemistry* 2009, **78:**477-513.
6. Dikic I: **Proteasomal and Autophagic Degradation Systems.***Annual review of biochemistry* 2017, **86:**193-224.
7. Keller JN, Huang FF, Markesbery WR: **Decreased levels of proteasome activity and proteasome expression in aging spinal cord.***Neuroscience* 2000, **98:**149-156.
8. Keller JN, Hanni KB, Markesbery WR: **Impaired proteasome function in Alzheimer's disease.***Journal of neurochemistry* 2000, **75:**436-439.

9. Oh S, Hong HS, Hwang E, Sim HJ, Lee W, Shin SJ, Mook-Jung I: **Amyloid peptide attenuates the proteasome activity in neuronal cells.***Mechanisms of ageing and development* 2005, **126:**1292-1299.
10. Sunkaria A, Yadav A, Bhardwaj S, Sandhir R: **Postnatal Proteasome Inhibition Promotes Amyloid-beta Aggregation in Hippocampus and Impairs Spatial Learning in Adult Mice.***Neuroscience* 2017, **367:**47-59.
11. XR J, KC C, YR C, TY L, CHA C, CL W, HC C: **Dysfunction of different cellular degradation pathways contributes to specific β-amyloid42-induced pathologies.***FASEB journal : official publication of the Federation of American Societies for Experimental Biology* 2018, **32:**1375-1387.
12. Verheijen BM, Stevens JAA, Gentier RJG, van 't Hekke CD, van den Hove DLA, Hermes D, Steinbusch HWM, Ruijter JM, Grimm MOW, Haupenthal VJ, et al: **Paradoxical effects of mutant ubiquitin on Abeta plaque formation in an Alzheimer mouse model.***Neurobiology of aging* 2018, **72:**62-71.
13. Tai HC, Serrano-Pozo A, Hashimoto T, Frosch MP, Spires-Jones TL, Hyman BT: **The synaptic accumulation of hyperphosphorylated tau oligomers in Alzheimer disease is associated with dysfunction of the ubiquitin-proteasome system.***The American journal of pathology* 2012, **181:**1426-1435.
14. Zhang JY, Liu SJ, Li HL, Wang JZ: **Microtubule-associated protein tau is a substrate of ATP/Mg(2+)-dependent proteasome protease system.***Journal of neural transmission (Vienna, Austria : 1996)* 2005, **112:**547-555.
15. Cripps D, Thomas SN, Jeng Y, Yang F, Davies P, Yang AJ: **Alzheimer disease-specific conformation of hyperphosphorylated paired helical filament-Tau is polyubiquitinated through Lys-48, Lys-11, and Lys-6 ubiquitin conjugation.***The Journal of biological chemistry* 2006, **281:**10825-10838.
16. de Poot SAH, Tian G, Finley D: **Meddling with Fate: The Proteasomal Deubiquitinating Enzymes.***Journal of molecular biology* 2017, **429:**3525-3545.
17. Lee BH, Lu Y, Prado MA, Shi Y, Tian G, Sun S, Elsasser S, Gygi SP, King RW, Finley D: **USP14 deubiquitinates proteasome-bound substrates that are ubiquitinated at multiple sites.***Nature* 2016, **532:**398-401.
18. Kim HT, Goldberg AL: **UBL domain of Usp14 and other proteins stimulates proteasome activities and protein degradation in cells.***Proceedings of the National Academy of Sciences of the United States of America* 2018, **115:**E11642-e11650.
19. Shin JY, Muniyappan S, Tran NN, Park H, Lee SB, Lee BH: **Deubiquitination Reactions on the Proteasome for Proteasome Versatility.***Int J Mol Sci* 2020, **21**.
20. Lee BH, Lee MJ, Park S, Oh DC, Elsasser S, Chen PC, Gartner C, Dimova N, Hanna J, Gygi SP, et al: **Enhancement of proteasome activity by a small-molecule inhibitor of USP14.***Nature* 2010, **467:**179-184.
21. Boselli M, Lee BH, Robert J, Prado MA, Min SW, Cheng C, Silva MC, Seong C, Elsasser S, Hatle KM, et al: **An inhibitor of the proteasomal deubiquitinating enzyme USP14 induces tau elimination in cultured neurons.***The Journal of biological chemistry* 2017, **292:**19209-19225.

22. Homma T, Ishibashi D, Nakagaki T, Fuse T, Mori T, Satoh K, Atarashi R, Nishida N: **Ubiquitin-specific protease 14 modulates degradation of cellular prion protein.***Scientific reports* 2015, **5:**11028.
23. Song Y, Li Z, He T, Qu M, Jiang L, Li W, Shi X, Pan J, Zhang L, Wang Y, et al: **M2 microglia-derived exosomes protect the mouse brain from ischemia-reperfusion injury via exosomal miR-124.***Theranostics* 2019, **9:**2910-2923.
24. Min JW, Lu L, Freeling JL, Martin DS, Wang H: **USP14 inhibitor attenuates cerebral ischemia/reperfusion-induced neuronal injury in mice.***Journal of neurochemistry* 2017, **140:**826-833.
25. Han KH, Kwak M, Lee TH, Park MS, Jeong IH, Kim MJ, Jin JO, Lee PC: **USP14 Inhibition Regulates Tumorigenesis by Inducing Autophagy in Lung Cancer In Vitro.***Int J Mol Sci* 2019, **20**.
26. Ma YS, Wang XF, Zhang YJ, Luo P, Long HD, Li L, Yang HQ, Xie RT, Jia CY, Lu GX, et al: **Inhibition of USP14 Deubiquitinating Activity as a Potential Therapy for Tumors with p53 Deficiency.***Mol Ther Oncolytics* 2020, **16:**147-157.
27. Wilson SM, Bhattacharyya B, Rachel RA, Coppola V, Tessarollo L, Householder DB, Fletcher CF, Miller RJ, Copeland NG, Jenkins NA: **Synaptic defects in ataxia mice result from a mutation in Usp14, encoding a ubiquitin-specific protease.***Nature genetics* 2002, **32:**420-425.
28. Jankowsky JL, Fadale DJ, Anderson J, Xu GM, Gonzales V, Jenkins NA, Copeland NG, Lee MK, Younkin LH, Wagner SL, et al: **Mutant presenilins specifically elevate the levels of the 42 residue beta-amyloid peptide in vivo: evidence for augmentation of a 42-specific gamma secretase.***Hum Mol Genet* 2004, **13:**159-170.
29. Zhang CE, Wei W, Liu YH, Peng JH, Tian Q, Liu GP, Zhang Y, Wang JZ: **Hyperhomocysteinemia increases beta-amyloid by enhancing expression of gamma-secretase and phosphorylation of amyloid precursor protein in rat brain.***The American journal of pathology* 2009, **174:**1481-1491.
30. Sun X, He G, Qing H, Zhou W, Dobie F, Cai F, Staufenbiel M, Huang LE, Song W: **Hypoxia facilitates Alzheimer's disease pathogenesis by up-regulating BACE1 gene expression.***Proceedings of the National Academy of Sciences of the United States of America* 2006, **103:**18727-18732.
31. Huang H, Guo M, Liu N, Zhao C, Chen H, Wang X, Liao S, Zhou P, Liao Y, Chen X, et al: **Bilirubin neurotoxicity is associated with proteasome inhibition.***Cell death & disease* 2017, **8:**e2877.
32. Gallyas F: **Silver staining of Alzheimer's neurofibrillary changes by means of physical development.***Acta morphologica Academiae Scientiarum Hungaricae* 1971, **19:**1-8.
33. Sun A, Nguyen XV, Bing G: **Comparative analysis of an improved thioflavin-s stain, Gallyas silver stain, and immunohistochemistry for neurofibrillary tangle demonstration on the same sections.***The journal of histochemistry and cytochemistry : official journal of the Histochemistry Society* 2002, **50:**463-472.
34. Ziyatdinova S, Gurevicius K, Kutchiashvili N, Bolkvadze T, Nissinen J, Tanila H, Pitkänen A: **Spontaneous epileptiform discharges in a mouse model of Alzheimer's disease are suppressed by antiepileptic drugs that block sodium channels.***Epilepsy research* 2011, **94:**75-85.
35. Kuo CL, Goldberg AL: **Ubiquitinated proteins promote the association of proteasomes with the deubiquitinating enzyme Usp14 and the ubiquitin ligase Ube3c.***Proceedings of the National Academy*

of Sciences of the United States of America 2017, **114:**E3404-e3413.

36. Huang H, Guo M, Liu N, Zhao C, Chen H, Wang X, Liao S, Zhou P, Liao Y, Chen X, et al: **Bilirubin neurotoxicity is associated with proteasome inhibition.***Cell Death and Disease* 2017, **8:**e2877.
37. Lee MS, Kao SC, Lemere CA, Xia W, Tseng HC, Zhou Y, Neve R, Ahlijanian MK, Tsai LH: **APP processing is regulated by cytoplasmic phosphorylation.***The Journal of cell biology* 2003, **163:**83-95.
38. Neddens J, Temmel M, Flunkert S, Kerschbaumer B, Hoeller C, Loeffler T, Niederkofler V, Daum G, Attems J, Hutter-Paier B: **Phosphorylation of different tau sites during progression of Alzheimer's disease.***Acta neuropathologica communications* 2018, **6:**52.
39. Chen Q, Yoshida H, Schubert D, Maher P, Mallory M, Masliah E: **Presenilin binding protein is associated with neurofibrillary alterations in Alzheimer's disease and stimulates tau phosphorylation.***The American journal of pathology* 2001, **159:**1597-1602.
40. Yuan C, Guo X, Zhou Q, Du F, Jiang W, Zhou X, Liu P, Chi T, Ji X, Gao J, et al: **OAB-14, a bexarotene derivative, improves Alzheimer's disease-related pathologies and cognitive impairments by increasing beta-amyloid clearance in APP/PS1 mice.***Biochim Biophys Acta Mol Basis Dis* 2019, **1865:**161-180.
41. Ito K, Arai K, Yoshiyama Y, Kashiwado K, Sakakibara Y, Hattori T: **Astrocytic tau pathology positively correlates with neurofibrillary tangle density in progressive supranuclear palsy.***Acta neuropathologica* 2008, **115:**623-628.
42. Rousseau A, Bertolotti A: **Regulation of proteasome assembly and activity in health and disease.***Nature reviews Molecular cell biology* 2018, **19:**697-712.
43. Paul S: **Dysfunction of the ubiquitin-proteasome system in multiple disease conditions: therapeutic approaches.***Bioessays* 2008, **30:**1172-1184.
44. Fitzpatrick AWP, Falcon B, He S, Murzin AG, Murshudov G, Garringer HJ, Crowther RA, Ghetti B, Goedert M, Scheres SHW: **Cryo-EM structures of tau filaments from Alzheimer's disease.***Nature* 2017, **547:**185-190.
45. Clavaguera F, Akatsu H, Fraser G, Crowther RA, Frank S, Hench J, Probst A, Winkler DT, Reichwald J, Staufenbiel M, et al: **Brain homogenates from human tauopathies induce tau inclusions in mouse brain.***Proceedings of the National Academy of Sciences of the United States of America* 2013, **110:**9535-9540.
46. Xie S, Jin N, Gu J, Shi J, Sun J, Chu D, Zhang L, Dai CL, Gu JH, Gong CX, et al: **O-GlcNAcylation of protein kinase A catalytic subunits enhances its activity: a mechanism linked to learning and memory deficits in Alzheimer's disease.***Aging cell* 2016, **15:**455-464.
47. Lee JH, Shin SK, Jiang Y, Choi WH, Hong C, Kim DE, Lee MJ: **Facilitated Tau Degradation by USP14 Aptamers via Enhanced Proteasome Activity.***Scientific reports* 2015, **5:**10757.
48. Feany MB, Jin YN, Chen P-C, Watson JA, Walters BJ, Phillips SE, Green K, Schmidt R, Wilson JA, Johnson GV, et al: **Usp14 Deficiency Increases Tau Phosphorylation without Altering Tau Degradation or Causing Tau-Dependent Deficits.***PLoS ONE* 2012, **7:**e47884.

49. Ortuno D, Carlisle HJ, Miller S: **Does inactivation of USP14 enhance degradation of proteasomal substrates that are associated with neurodegenerative diseases?** *F1000Research* 2016, **5:**137.

Figures

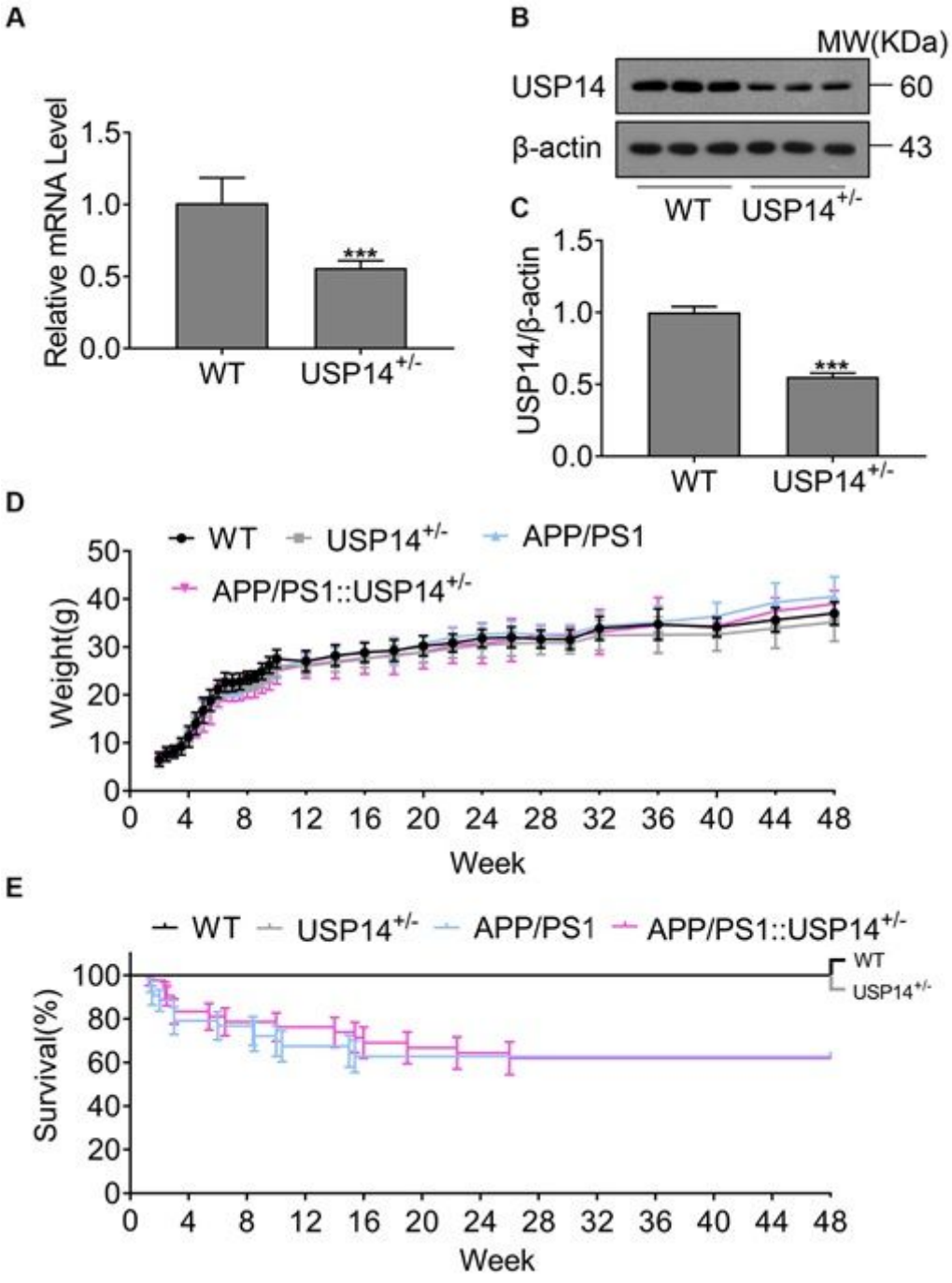

Figure 1

Baseline characterization of USP14+/- mice. (A) The qRT-PCR results of USP14 in WT and USP14+/- mouse cortex; (B and C) Representative images (B) and pooled densitometry data (C) of Western blot analyses for USP14 in WT and USP14+/- mouse cortex; ***p<0.001 vs. WT, n=3 mice). (D) Time course of changes in mouse body weight during postnatal 48 weeks. (E) Kaplan-Meier survival analyses for mice of

the indicated genotypes during postnatal 48 weeks. All premature death of the APP/PS1 mice took place before reaching 26 weeks of age; the introduction of USP14+/- did not change the mortality of APP/PS1 mice; a cohort of 32 WT, 29 USP14+/-, 32 APP/PS1, and 34 USP14+/-::APP/PS1 mice were included.

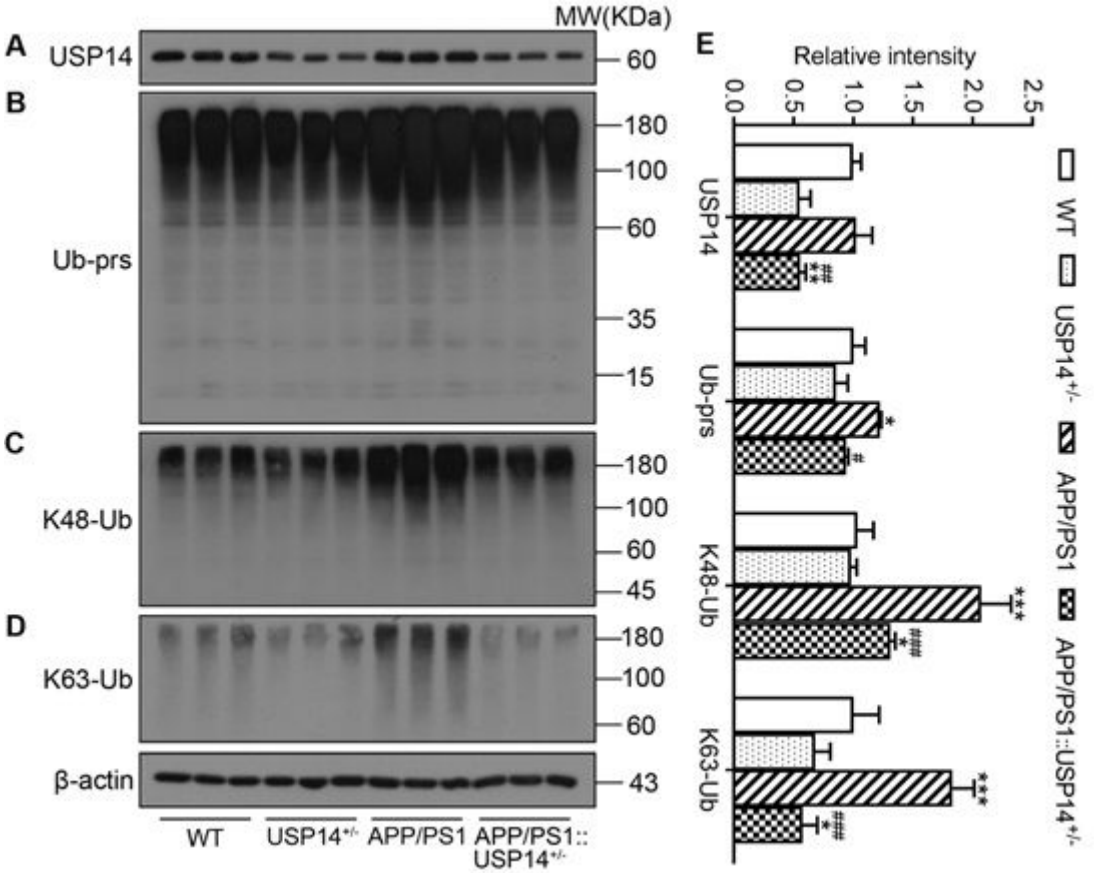

Figure 2

Changes in protein abundance of USP14 and ubiquitinated proteins in the cerebral cortex of mice with the indicated genotypes.Proteins were extracted from the cerebral cortex tissue samples from 12-month-old mice and subjected to SDS-PAGE and Western blot analysis for the indicated proteins. Shown are the representative images of Western blot analyses for USP14 (A), total ubiquitinated proteins (Ub-Prs, B), K48-linked Ub conjugates (C), K63-linked Ub conjugates (D), as well as the pool densitometry data of each of them (E).β-Actin was probed as loading control. N=6, *P<0.05, **P<0.01, and ***P<0.001 vs. WT； #P<0.05, ##P<0.01, and###P<0.001 vs. APP/PS1;1-way ANOVA followed by the Holm-Sidak test for pair-wise comparisons.

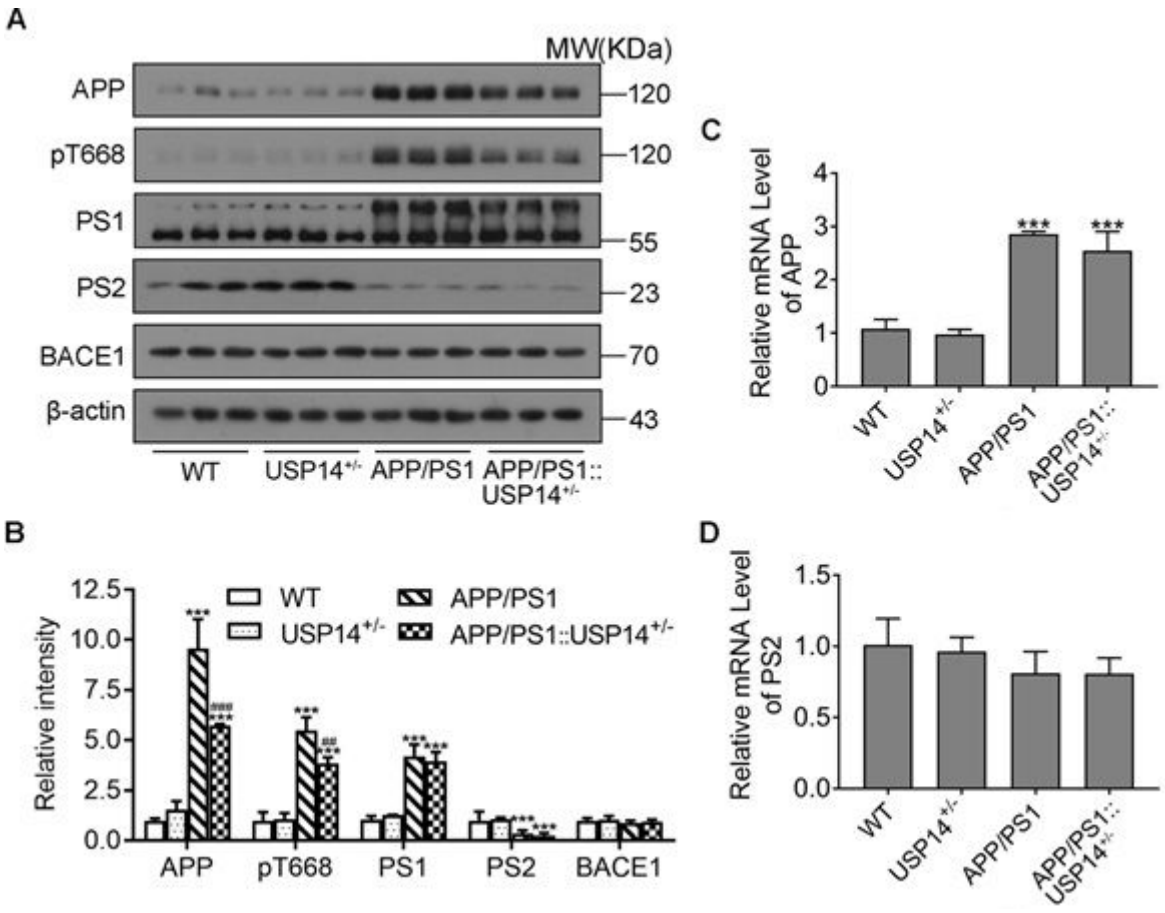

Figure 3

The effect of USP14 haploinsufficiency on the expression of APP and APP processing enzymes in the cerebral cortex of WT and APP/PS1 mice. Protein and RNA were extracted from the cerebral cortex tissue samples of 12-month-old mice of the indicated genotypes. (A, B) Representative images (A) and pooled densitometry data of Western blot analyses for the indicated proteins. (C, D) The RT-qPCR results of APP (C) and PS2 (D) in cerebral cortex in each group. N=6, *P<0.05, ***P<0.001 vs. WT; #P<0.05, ###P<0.001 vs. APP/PS1; 1-way ANOVA followed by the Holm-Sidak test for pair-wise comparisons.

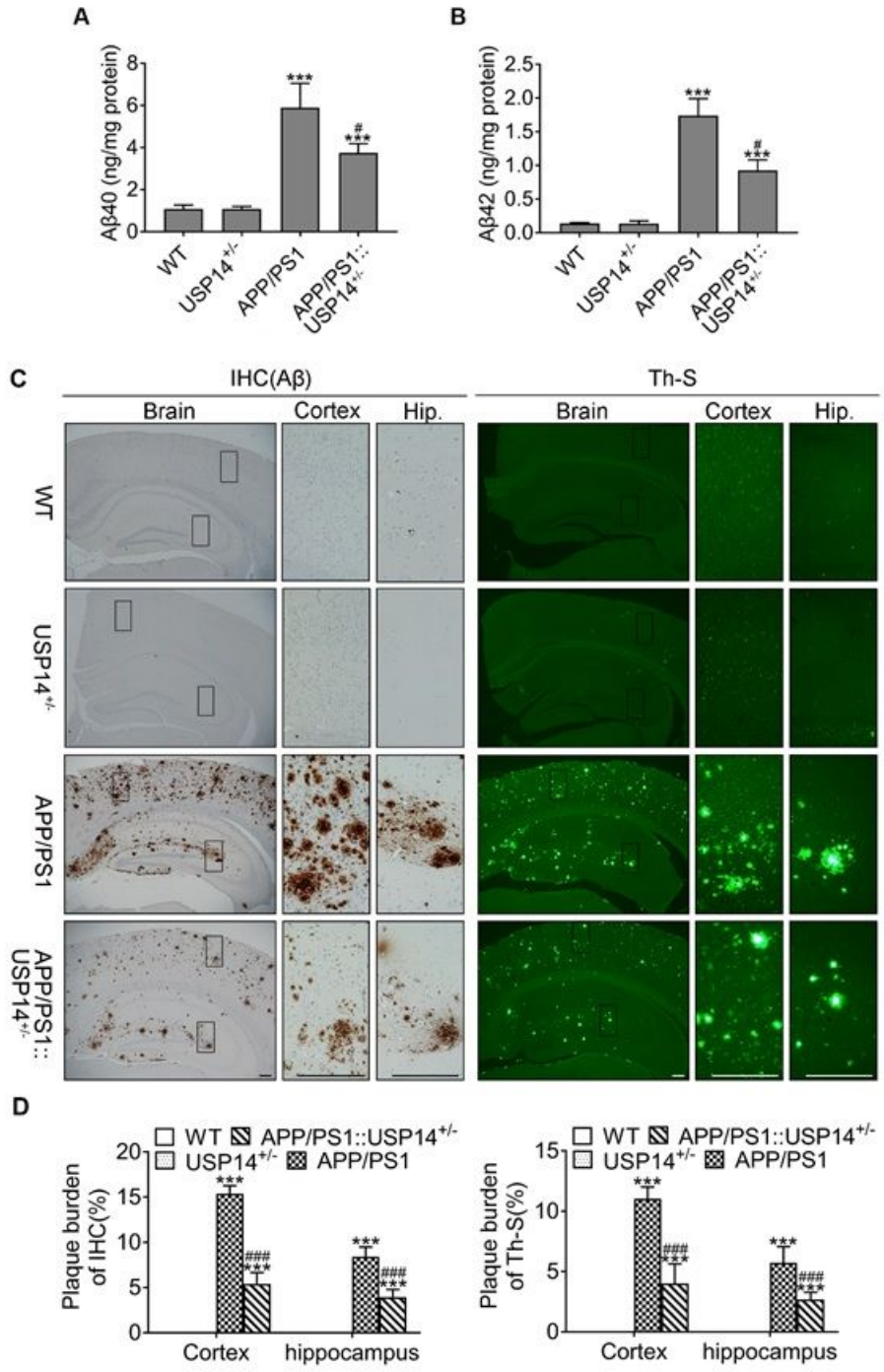

Figure 4

Effects of USP14 haploinsufficiency on Aβ deposition.(A and B) The content of Aβ40 (A) and Aβ42 (B) in the hippocampal tissues of all genotypes of mice at 12 months as assessed with ELISA; ***P<0.001 vs. WT; #P<0.05 vs. APP/PS1; n=3 mice/group. (C) Representative images of immunohistochemical staining for Aβ (IHC(Aβ); left panel) and the thioflavin-s staining (Th-S) amyloid plagues (right panel) in the cerebral cortex and hippocampus of mice with the indicated genotypes. Bar=200 μm, n=3). (D) Optical

density analysis of the amyloid plaque area as illustrated in Panel C. ***P<0.001 vs. WT;###P<0.001 vs. APP/PS1; n=3 mice/group.

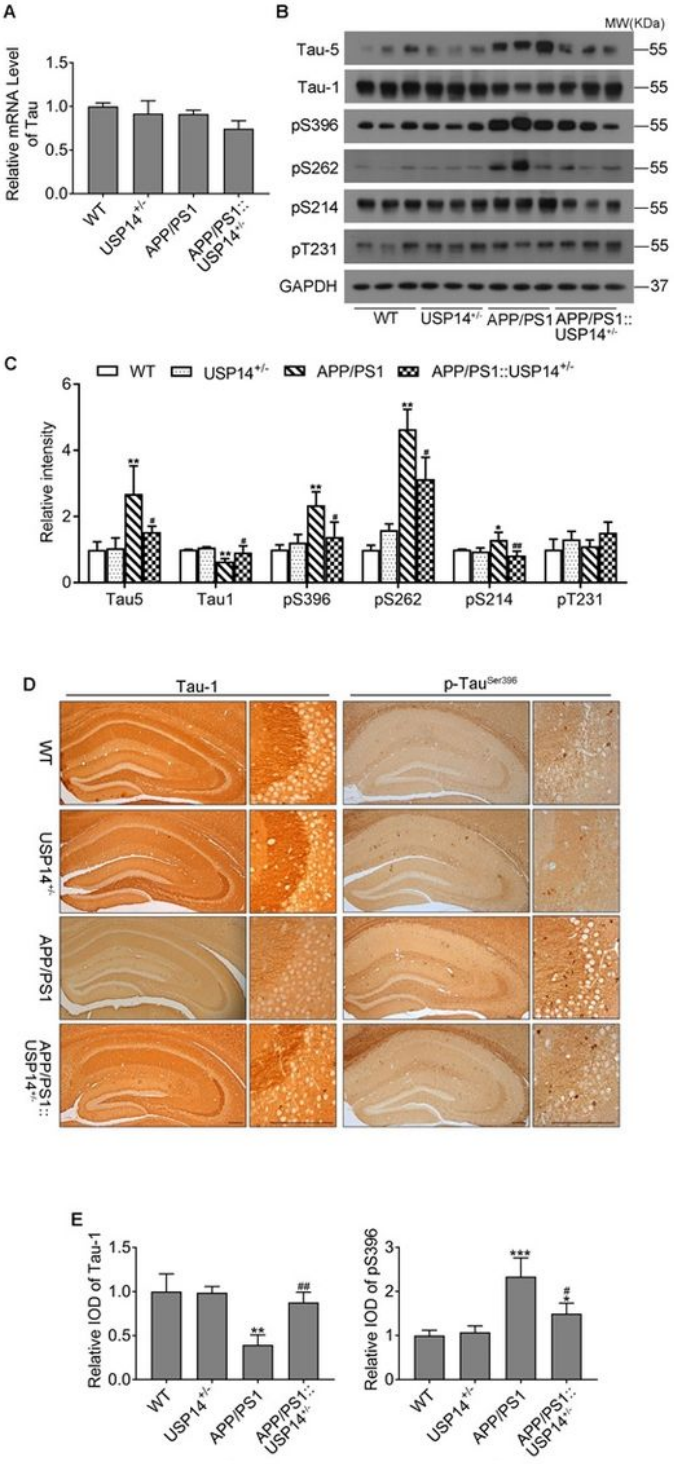

Figure 5

Effects of USP14 haploinsufficiency on Tau expression in the hippocampus. Hippocampal tissue samples from 12-month-old mice of the indicated genotypes were used for extraction of total proteins or RNAs or were subjected to fixation and subsequent immunohistochemistry staining. (A) qRT-PCR results

of Tau mRNA levels. (B and C) Representative images (B) and pooled densitometry data (C) of the Western blot analyses for total Tau proteins (Tau-5), Ser195/198/199/202- dephosphorylated Tau (Tau-1), as well as Ser396-, Ser262-, Ser214-, or Thr231- phosphorylated Tau (pS396, pS262, pS214, or pT231, respectively). *P<0.05, **P<0.01 vs. WT;#P<0.05, ##P<0.01 vs. APP/ PS1, n=6). (D and E) representative images (D) and pooled optical density (E) of the immunohistochemical analyses for Tau-1 and pS396-Tau in hippocampal tissues. Bar=200 μm; *P<0.05, **P<0.01 vs. WT; #P<0.05, ##P<0.01 vs. APP/ PS1; n=3 mice/genotype.

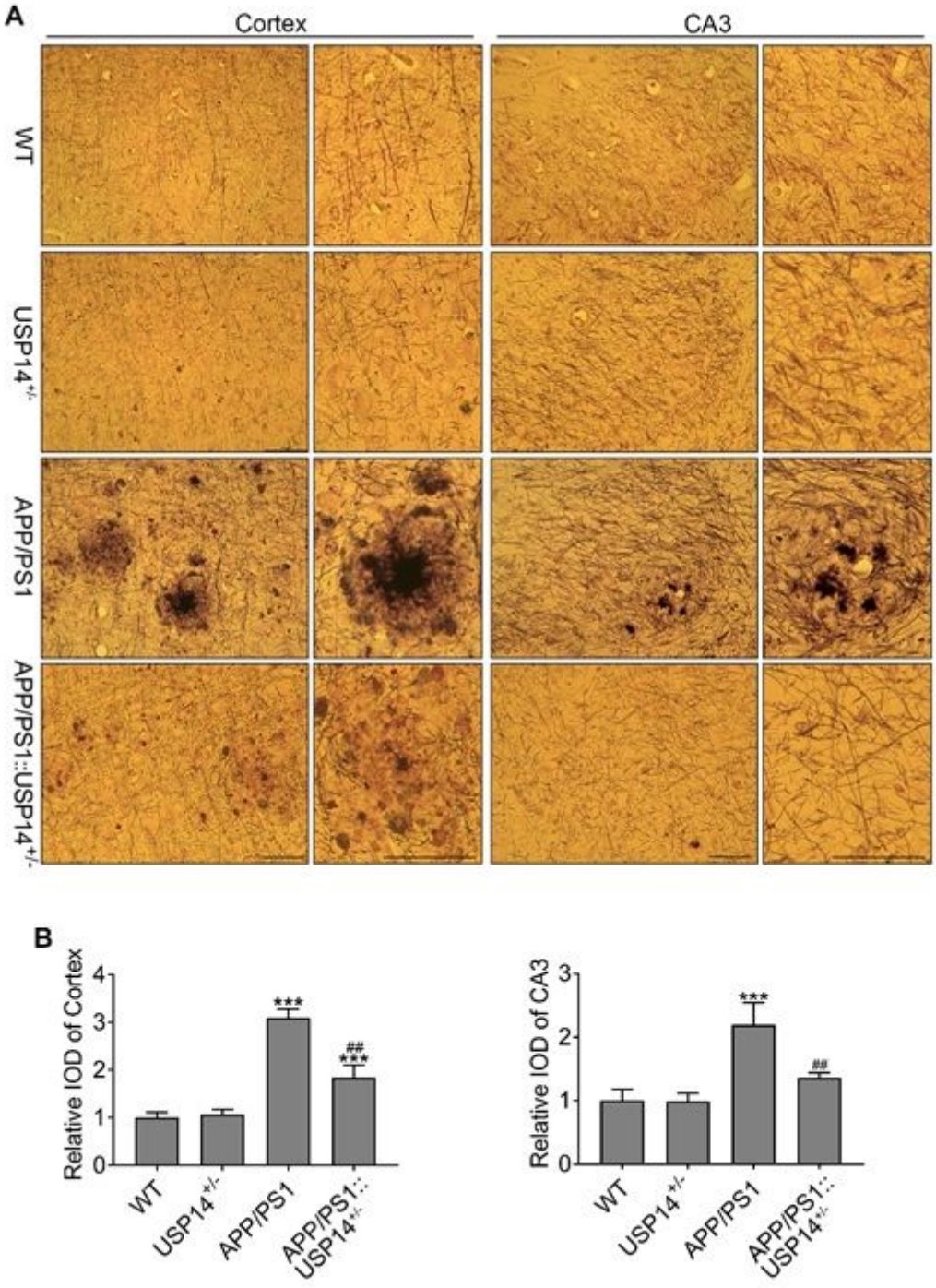

Figure 6

USP14 haploinsufficiency ameliorates the senile plaques and neurofibrillary tangles in AD mice. (A) Representative images of theGallyas-Braak silver staining of tissue sections from the cerebral cortex (left panel) and the CA3 region of hippocampus (right panel). Scale Bar =50 μm. (B) Optical density analysis of images as illustrated in Panel A. IOD value was **P<0.01, ***P<0.001 vs. WT; ##P<0.01 vs. APP/ PS1; n=3 mice/group.

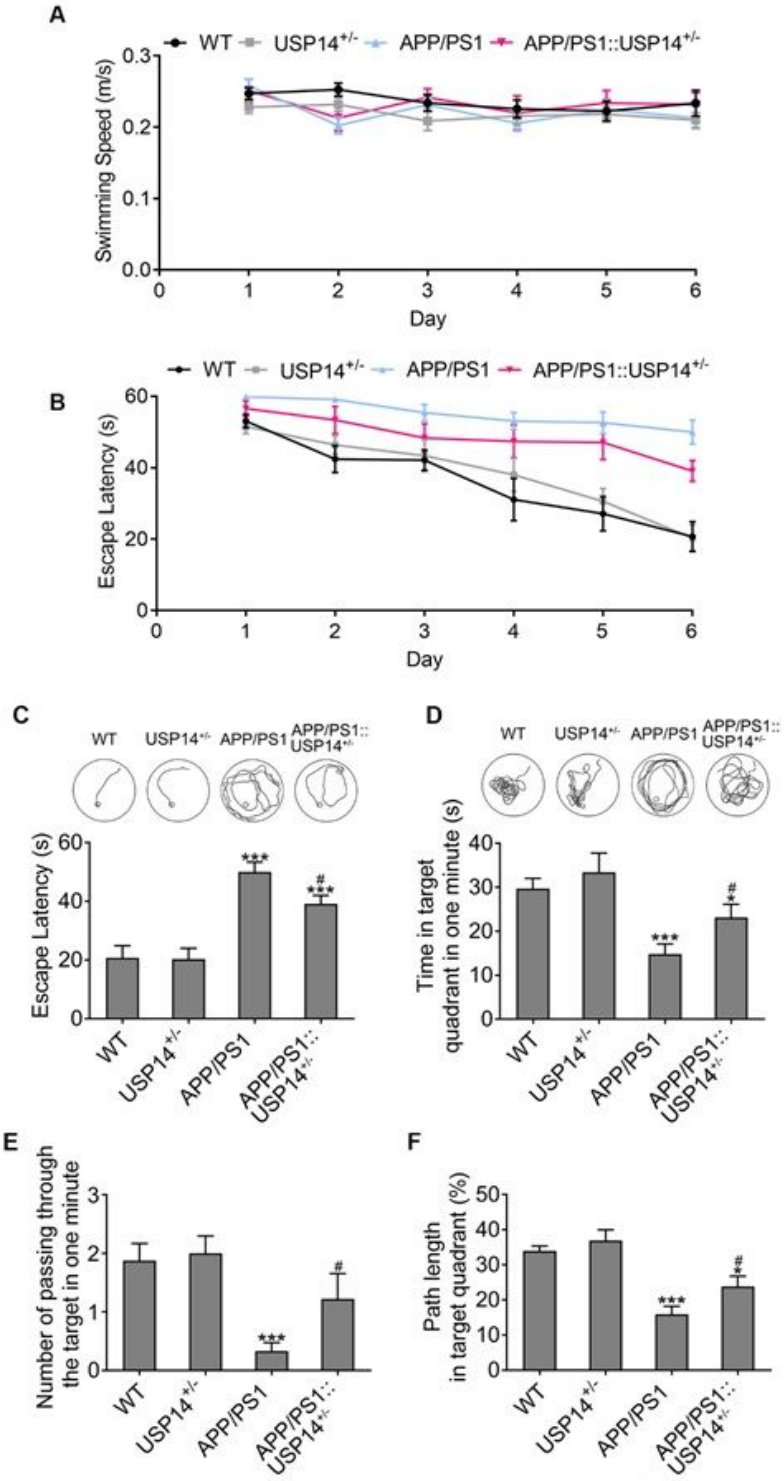

Figure 7

USP14 haploinsufficiency improves learning and memory impairment of aging APP/PS1 mice. Mice of the indicated genotypes at 12 months of age were subjected to Morris water maze tests. (A) Comparison of the average swimming speed among the 4 groups during the test. (B) Changes in the escape latency in Morris water maze training; (C) Comparison of the escape latency and representative track of mice of different genotypes on the sixth day of Morris water maze training. (D-F) The representative track and the time in the platform quadrant (D), the number of crossing the platform (E) and the percentage of target quadrant swimming distance to the total distance (F) in each group within 1min after withdraw the platform on the eighth day. *P<0.05, ***P<0.001 vs. WT; #P<0.05, ###P<0.001 vs. APP/PS1; n = 15 WT, 15 USP14+/-, 12 APP/PS1, 10 APP/PS1::USP14+/- mice.

Supplementary Files

This is a list of supplementary files associated with this preprint. Click to download.

- TableS1.pdf